

## The inclination of magnetic dipole effect and nanoscale exchange of heat of the Cross nanofluid

Thongchai Botmart, Syed Zahir Hussain Shah, Zulqurnain Sabir, Wajaree weera, R. Sadat, Mohamed R. Ali & Wael Al-Kouz

To cite this article: Thongchai Botmart, Syed Zahir Hussain Shah, Zulqurnain Sabir, Wajaree weera, R. Sadat, Mohamed R. Ali & Wael Al-Kouz (2022): The inclination of magnetic dipole effect and nanoscale exchange of heat of the Cross nanofluid, *Waves in Random and Complex Media*, DOI: [10.1080/17455030.2022.2128225](https://doi.org/10.1080/17455030.2022.2128225)

To link to this article: <https://doi.org/10.1080/17455030.2022.2128225>



Published online: 29 Sep 2022.



Submit your article to this journal [↗](#)



View related articles [↗](#)



View Crossmark data [↗](#)



# The inclination of magnetic dipole effect and nanoscale exchange of heat of the Cross nanofluid

Thongchai Botmart<sup>a</sup>, Syed Zahir Hussain Shah<sup>b</sup>, Zulqurnain Sabir<sup>b</sup>, Wajaree weera<sup>a</sup>, R. Sadat<sup>c</sup>, Mohamed R. Ali <sup>d,e</sup> and Wael Al-Kouz<sup>f</sup>

<sup>a</sup>Faculty of Science, Department of Mathematics, Khon Kaen University, Khon Kaen, Thailand; <sup>b</sup>Department of Mathematics and Statistics, Hazara University, Mansehra, Pakistan; <sup>c</sup>Faculty of Engineering, Department of Mathematics, Zagazig University, Zagazig, Egypt; <sup>d</sup>Faculty of Engineering and Technology, Future University, Cairo, Egypt; <sup>e</sup>Basic Engineering Mathematics Department, Benha Faculty of Engineering, Benha University, Egypt; <sup>f</sup>College of Engineering and Technology, American University of the Middle East, Egaila, Kuwait

## ABSTRACT

Nanoscale energy exchange and movement of fluid by Lorentz force is the most recent problem that has a strong connection with applied mathematics due to the consumption of energy. Imposing the inclination of Magnetic dipole in the fluid has abundant applications in magnetic drug engineering, astrophysics, sensors, geophysics, cosmology, and targeting. This study is associated with the exchange of energy under the influence of the inclination of Magnetic dipole with cylinder geometry. The Cross nanofluid mathematical model is launched to carry the nanoscale energy exchange with temperature-dependent thermal conductivity. The permeable cylinder geometry along with the different effects is provided during the expanding/contracting cylinder. Whereas Cross fluid helps to investigate the problem in shear thinning/thickening regions. The numerical representations of the problem are provided via the BVP4C scheme.

## ARTICLE HISTORY

Received 8 December 2021  
Accepted 19 September 2022

## KEYWORDS

Cross nanofluid; heat transport at nanoscale; Lorentz force effect; temperature-dependent conductivity; BVP4C

## Nomenclature

$b_0$	Constant of dimension length. $t$
$K(T)$	Variable thermal conductivity
$\beta$	Constant of contraction – expansion
$U_w(x, t)$	Initial velocity
$U_e(x, t)$	Free stream velocity
$T_w, C_w$	Temperature and concentration of the cylinder
$T_\infty, C_\infty$	Temperature and concentration of the cylinder
$a, c$	Constant of dimension $(time)^{-1}$
$\tau$	Cauchy stress tensor
$k$	Thermal conductivity
$x, r$	Space variable
$s$	Suction parameter

**CONTACT** Mohamed R. Ali  mohamed.reda@bhit.bu.edu.eg

$k_{\infty}$	Conductivity away for
$Pr$	Prandtl number
$\xi$	Chemical rate reaction parameter
$\lambda$	Velocity ratio parameter
$\mu_0$	zero shear rate viscosity
$A_1$	First Rivlin Erickson's tensor
$\mu_{\infty}$	Infinite shear rate viscosity
$p$	Pressure
$I$	Identity tensor
$\Gamma$	Relaxation time constant
$n$	Power law index
$Sc$	Schmidt number
$\mu$	Viscosity
$q_w$	Wall shear stress
$\tau_{rx}$	Heat flux
$M$	Magnetic parameter
$u, v$	Velocity component
$c_f$	Skin friction
$B_0$	Magnetic field strength constant
$\dot{\gamma}$	Shear strain
$B$	Magnetic field strength
$c_p$	Specific heat
$D$	Solute Diffusivity
$R_r$	Chemical reaction parameter
$\sigma$	Reaction rate parameter
$\rho$	Density
$C$	Concentration profile
$T$	Temperature profile
$V$	Velocity profile
$\theta_w$	Temperature ratio parameter
$A$	Unsteadiness parameter
$We$	Weissenberg
$\alpha_m$	Thermal diffusivity
$Re$	Reynold number
$Nu$	Nusselt number

## 1. Introduction

The technology and thermal engineering fields have been facing energy consumption problems for many decades. These energy consumptions can be handled to increase the thermal conductivity of nanoliquids. Nanoscale heat transport is very effective for this purpose by considering nanofluids. The Nanoscale process of heat transport is utilized for minimizing emerging energy issues. The formation of fluid is done by imposing the bombardment of solid particles. Consequently, the obtained nanoparticles have less than 100 nm dimension are called nanofluids. Nanofluid is a stream of all nanoparticles and boosts energy performance by increasing thermal conductivity. To make better energy

performance by increasing the thermal conductivity is considered an advance and valid procedure. Recently, many scholars worked on nanofluid and nanoscale heat transport. Viscoelastic nanofluid with imposed external buoyancy forces was explored by Waqas et al. [1]. The flow optimization with SiC/EG-water nanofluids and heat transfer analysis was made by Yang et al. [2]. The prediction of heat transport using thermal conductivity was explored by Komeilibirjandi et al. [3]. Yang et al. [4] addressed the air purification and heat recovery phenomenon with the highlights of nanofluids. Puneeth et al. [5] considered an effective hybrid nanofluid with the effects of bioconvection and radiation of heterogeneous – homogeneous chemical reactions.

The association of the magnetic fields and their related properties based on their fluid mechanism is known as magnetohydrodynamics (MHD). A magnetic field creates electricity and force, which, combining current and magnetic effect, is called Lorentz force. The phenomenon of MHD has various real-life applications, such as electric power generation systems, development of high-efficiency, contamination and determination of ECG signal, magneto resonance imaging (MRI), incrementing the amplitude of the T wave, molten metal, metal transformation procedure, nanofluid pumping, solid-state mixtures, pumping of seawater, fluid pumping, the industry of crystal growing, industry of polymers, MHD accelerations, MHD thrusters, MHD generator/motor, and flow control around hypersonic [6–17]. The theory related to MHD depicts the influence of magnetic effects. The Lorentz force is generated due to the effects of fluid motion. Keeping in view of the vital effects of the magnetic dipole on fluid motion, many scholars contributed by placing perpendicular/inclined magnetic dipole over fluid flow. The gyrotactic motile microorganism with Cross nanofluid and unsteady MHD aspect of flow over the geometry of a heated sheet was discovered by Reddy et al. [18]. Bioconvection, nonlinear thermal radiation, and melting process over wedge geometry were depicted by Waqas et al. [19]. Thermal conductivity performance to boost the heat transfer and magneto effect with cylinder-constructed geometry was numerically achieved by Imran et al. [20]. Furthermore, Noor et al. [21,22] worked on MHD viscous flow over a linearly stretching sheet embedded in a non-Darcian porous medium and they presented the numerical results with attached physical parameters.

Furthermore, the saturated flow of Cross nanofluid and its dynamics of multiple solutions attached facts of heat source effects and cross-diffusion were found numerical by [21,22].

Chemical reactions diverted human's life from tease to ease. It made human life very easy and there is no world progress without chemical reactions. There is a need for minimum energy, which activates the chemical reaction known as activation energy. A chemical reaction, which remains fixed during the process, is called a homogeneous chemical process. On the other hand, a chemical process is able to occur everywhere, which is referred to a heterogeneous chemical process. Physically, there are two types of chemical processes, one is a constructive chemical process and the other one is a destructive process. In fluid mechanism, chemical reaction and Activation energy are utilized to judge the mass transport of fluid. According to many investigations, the chemical process plays a vital role in the mass transport of fluid. Xiong et al. [23] worked on the dynamics of Cross nanofluid and its multiple solutions with the geometry of thin needlepoint. The same work related to the dual solution with the addition of external buoyancy force was pointed out by Hafeez et al. [24]. Chemical reaction process and heat sink/source effect of nanofluid and their numerical outcomes are displayed in the scientific community by Li et al. [25]. Chemical reactions help

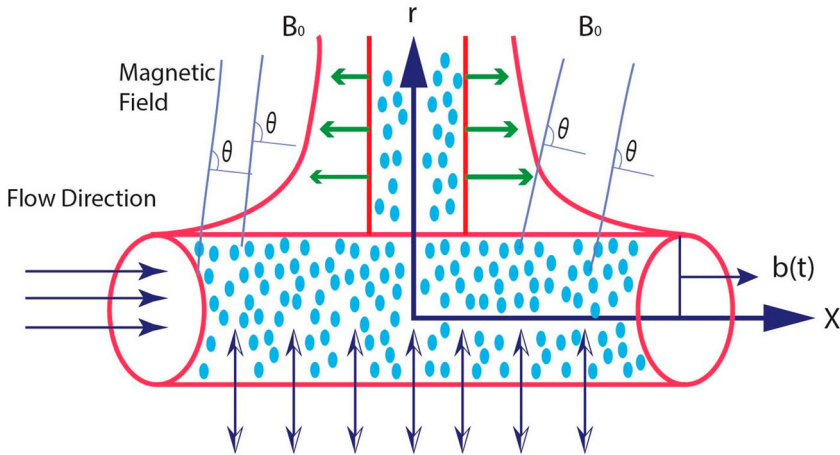


**Figure 1.** The geometry of flow in the permeable cylinder.

with autocatalytic and heterogeneous catalysis over the physical shape of a rotating disk as shown by Yu et al. [26]. Furthermore, Yu et al. [26] considered Ostwald-de-Waele nanofluid over rotating disk geometry with heterogeneous catalysis. MHD hybrid nanofluid with the feature of multiple slips with the facts of the autocatalytic chemical process along with the Cattaneo – Christov heat flux was discovered by Gul et al. [27] and others [28–33].

This article presents the numerical judgment of energy exchange and inclination of magnetic dipole effects on time-dependent Cross nanofluid with cylinder geometry. The viscosity of the Cross nanofluid model is utilized to obtain the numerical results of nanoscale energy exchange and temperature-dependent variable thermal conductivity. Permeable cylinder geometry represents the effect of several parameters during the expanding/contracting cylinder and the Cross fluid helps to investigate the problem in shear thinning/thickening region.

## 2. Geometry of flow in the permeable cylinder and problem formulation

The flow is passing through the permeable cylinder with the competence of extraction/expansion, whose time dependent radius is  $b(t) = (1 - \beta t)^{1/2} b_0$ , where  $b_0$  is a positive constant and  $\beta$  is a constant of contraction/expansion with positive and negative values.  $U_w(x, t) = \frac{2cx}{1-\beta t}$  in mathematics is called time-dependent stretching/shrinking velocity and  $U_e(x, t) = \frac{2ax}{1-\beta t}$  is the free stream velocity. The stagnation point is also considered in the cylinder geometry at  $r = b_0$ , with  $x = 0$ . The inclined magnetic field  $B(t) = \frac{\beta_0}{\sqrt{(1-\beta t)}}$  is imposed in the radial direction of the cylinder. Passing flow through the cylinder is considered 2D and incompressible. Surface temperature, surface concentration, ambience temperature, and ambience concentration of cylinder denoted by  $T_w, C_w, T_\infty, C_\infty$  and  $T_w > T_\infty$ . Figure 1

A tensor of the Cross model and all its related mathematics are listed in Equations (1) and (2).

$$\tau = -pI + \mu(\dot{\gamma})A_1.$$

$$\mu(\dot{\gamma}) = \left[ \mu_\infty + \frac{\mu_0 - \mu_\infty}{1 + (\Gamma \dot{\gamma})^n} \right]. \quad (1)$$

$$\left( \dot{\gamma} = \sqrt{\frac{1}{2} \text{tr}(A_1)^2}, \quad A_1 = (\nabla V) + (\nabla V)^T \right). \quad (2)$$

The velocity assumption is taken as

$$V = [u(r, x, t), v(r, x, t), 0], T = T(r, x, t), C = C(r, x, t). \quad (3)$$

The boundary layer analysis (BLA) and formulated problem take the following mathematical form:

$$\frac{\partial(ru)}{\partial x} + \frac{\partial(rv)}{\partial x} = 0, \quad (4)$$

$$\begin{aligned} \frac{\partial u}{\partial t} + u \frac{\partial u}{\partial x} + v \frac{\partial u}{\partial r} = U_e \frac{\partial U_e}{\partial x} + \frac{v}{r} \frac{\partial u}{\partial r} \left[ \frac{1}{\left[ \left( 1 + \Gamma \frac{\partial u}{\partial r} \right)^n \right]} \right] + \frac{\partial U_e}{\partial t}, \\ + v \frac{\partial}{\partial r} \left[ \frac{\frac{\partial u}{\partial r}}{\left[ \left( 1 + \Gamma \frac{\partial u}{\partial r} \right)^n \right]} \right] + \frac{\sigma B^2(t)}{\rho} \sin^2(\varpi) (u - U_e), \end{aligned} \quad (5)$$

$$\left[ \frac{\partial T}{\partial t} + v \frac{\partial T}{\partial r} + u \frac{\partial T}{\partial x} \right] = k \frac{1}{r} \frac{\partial}{\partial r} \left[ k(T) r \frac{\partial T}{\partial r} \right], \quad (6)$$

$$\left( \frac{\partial C}{\partial t} + v \frac{\partial C}{\partial r} + u \frac{\partial C}{\partial x} \right) = D \left[ \frac{\partial^2 C}{\partial r^2} + \frac{1}{r} \frac{\partial C}{\partial r} \right], \quad (7)$$

The associated boundary conditions (BCs) are

$$u = U_w(x, t) = \frac{2cx}{1 - \beta t}, v = V_w(t) = -\frac{ab_0 s}{\sqrt{1 - \beta t}},$$

$$T = T_w, C = C_w \text{ at } r = b(t), \quad (8)$$

$$r \rightarrow \infty, C \rightarrow C_\infty, T \rightarrow T_\infty, u \rightarrow U_e(x, t), \quad (9)$$

$$K(T) = k_\infty \left( 1 + \varepsilon \left( \frac{T - T_\infty}{T_w - T_\infty} \right) \right), \quad (10)$$

$$u = \frac{2ax}{(1 - \beta t)} f'(\eta), v = -\frac{ab_0}{(1 - \beta t)} \frac{f(\eta)}{\sqrt{\eta}}, \quad \eta = \left( \frac{a_0}{r} \right)^{-2} (1 - \beta t)^{-1}.$$

$$\theta(\eta) = \frac{T - T_\infty}{T_f - T_\infty}, \phi(\eta) = \frac{C - C_\infty}{C_f - C_\infty}, \quad (11)$$

$$\begin{aligned} \eta(1 + (1 - n)We^n(f'')n)f'' + (2 + (1 - n)We^n(f'')n)\frac{1}{2}f'' \\ + Re(ff'' - f'^2 + 1)(1 + We^n(f'')n)^2 - A(\eta f'' + f' - 1)(1 + We^n(f'')n)^2 \\ - M^2 \sin^2(\varpi) Re(1 + We^n(f'')n)^2 (f' - 1) = 0, \end{aligned} \quad (12)$$

$$(1 + \varepsilon\theta)\eta\theta'' + (1 + \varepsilon\theta)\theta' + \varepsilon\eta\theta'^2 - PrA\eta\theta' - PrRef\theta' = 0, \quad (13)$$

$$\eta\phi'' + \phi' - ASc\eta\phi' + ReScf'\phi' - ReScB^*\phi = 0, \quad (14)$$

The BCs related to the above system of ODEs are given as follows:

$$\begin{aligned}\phi(1) = 1, f'(1) = \lambda, f(1) = s, \theta(1) = 1, \\ \text{as } \eta \rightarrow \infty, \theta(\eta) \rightarrow 0, f'(\eta) \rightarrow 1, \phi(\eta) \rightarrow 0,\end{aligned}\quad (15)$$

$$\begin{aligned}Re = \frac{ab_0^2}{2\nu}, A = \frac{\beta b_0^2}{4\nu}, Sc = \frac{\nu}{D}, Pr = \frac{\nu}{\alpha_m}, \\ We = \frac{4r\Gamma U_e}{b_0(1-\beta t)}, \xi = \frac{R_r(1-\beta t)}{2a}, M^2 = \frac{\sigma\beta_0^2}{2\rho a}, \theta_w \\ = \frac{T_w}{T_\infty}, \lambda = \frac{c}{a},\end{aligned}\quad (16)$$

Flow mechanism and transformation of heat are the Nusselt numbers  $Nu$  and the local skin friction coefficient  $C_f$  is given as follows:

$$Nu = \frac{b(t)q_w|_{r=b(t)}}{2k(T_w - T_\infty)} \text{ and } C_f = \frac{\tau_{rx}|_{r=b(t)}}{\frac{1}{2}\rho U_e^2}, \quad (17)$$

$q_w$  is the wall heat flux for shear stress,  $\tau_{xx}$  represents the wall shear stress, and both are defined as follows:

$$\tau_{xx} = \mu_0 \frac{\partial u}{\partial r} \left[ \frac{1}{1 + \Gamma^n \left( \frac{\partial u}{\partial r} \right)^n} \right]_{r=b(t)}, q_w = -k \frac{\partial T}{\partial r} |_{r=b(t)}, \quad (18)$$

The Nusselt number  $Nu$  and the local skin friction coefficient  $C_f$  taken the following form:

$$\begin{aligned}Nu = -\theta'(1) \\ C_f Re \frac{x}{b(t)} = f''(1) \left[ \frac{1}{1 + We^n (f''(1))^n} \right],\end{aligned}\quad (19)$$

### 3. Methodology for Bvp4c

Nonlinear systems of ODEs attached with boundary conditions (BCs) are shot down into the system of linear equations with initial conditions (ICs). The methodology is illustrated as under

$$\begin{aligned}F = l_1, l'_1 = l_2, l'_2 = l_3, \\ y'_3 = \frac{1}{\eta(1 + (1-n)We^n(l_3)^n)} \times \left[ \begin{array}{l} -(2 + (1-n)We^n(l_3)^n) \frac{1}{2} l_3 \\ -Re(l_1 l_3 - l_2^2 + 1)(1 + We^n(l_3)^n)^2 \\ + A(\eta l_3 + l_2 - 1)(1 + We^n(l_3)^n)^2 \\ + M^2 \sin^2(\varpi) Re(1 + We^n(l_3)^n)^2 (l_2 - 1) = 0, \end{array} \right] \\ l_4 = \theta, l'_4 = l_5 \\ l'_5 = \frac{1}{(1 + \varepsilon l_4)\eta} \left[ PrA\eta l_5 + PrRe l_1 l_5 - (1 + \varepsilon l_4)l_5 - \varepsilon \eta (l_5)^2 \right]\end{aligned}$$

Furthermore, the concentration form is written as follows:

$$l_6 = \phi, l_6' = l_7$$

$$y_7' = \frac{1}{\eta} [ASc\eta l_7 - l_7 - ReSc l_2 l_7 + ReSc B l_6]$$

Now the initial conditions are written as follows:

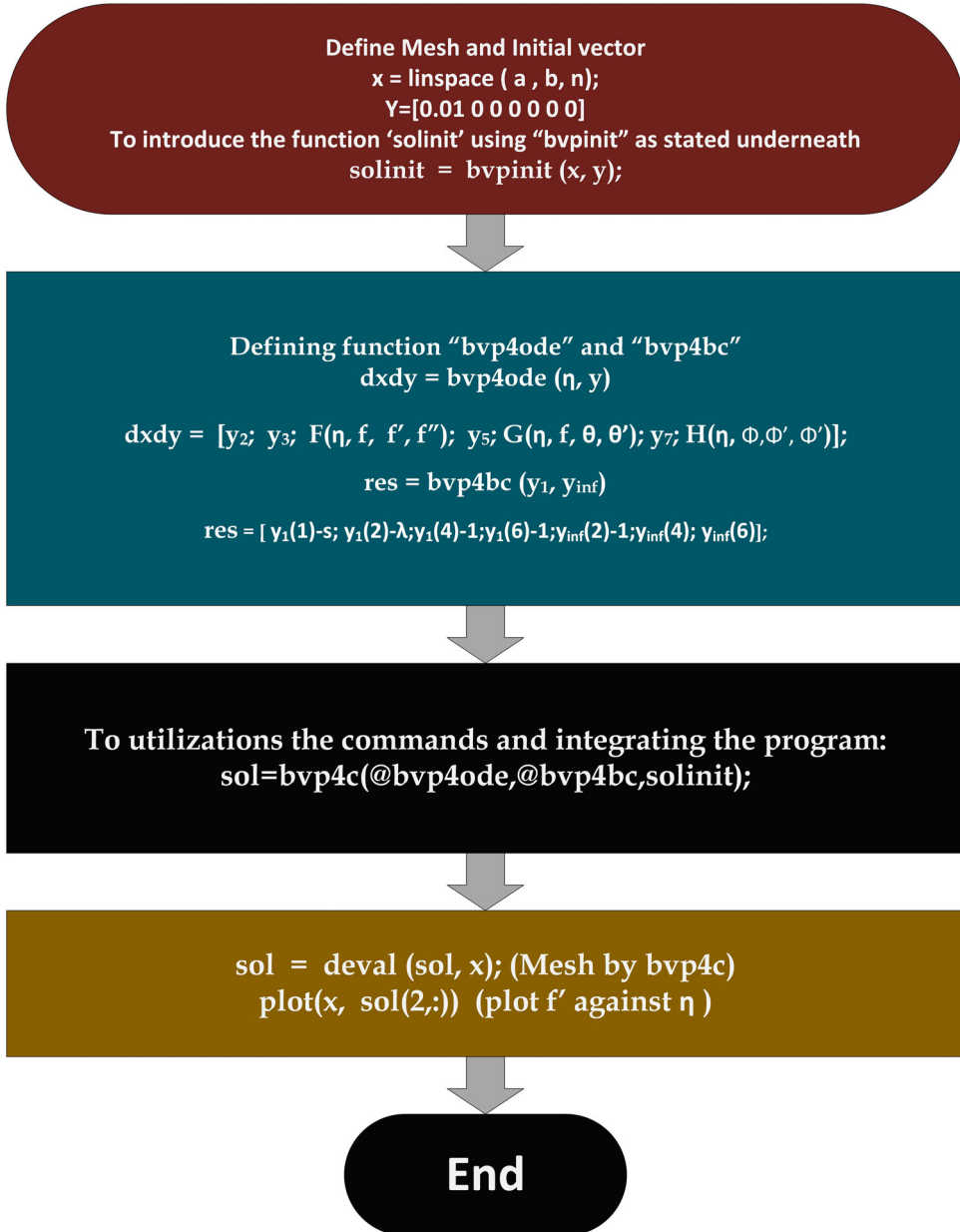


Chart 1. Methodology.



$$l_6(1) = 1, l_2(1) = \lambda, l_1(1) = s, l_4(1) = 1,$$

$$\text{as } \eta \rightarrow \infty, l_4(\eta) \rightarrow 0, l_2(\eta) \rightarrow 1, l_6(\eta) \rightarrow 0,$$

#### 4. Methodology for Keller Box

Chart 1 and 2

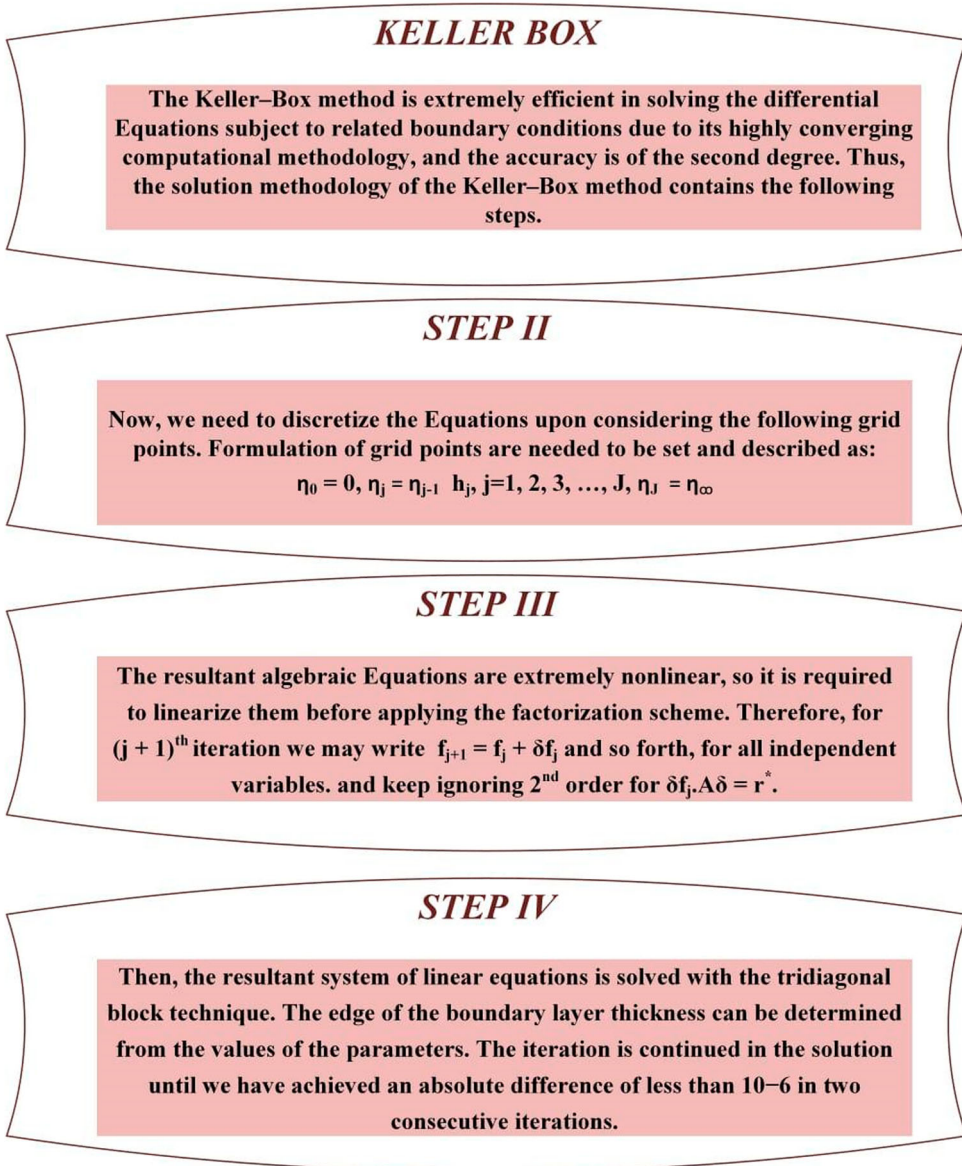


**Chart 2.** Complete demonstration for the Keller box.

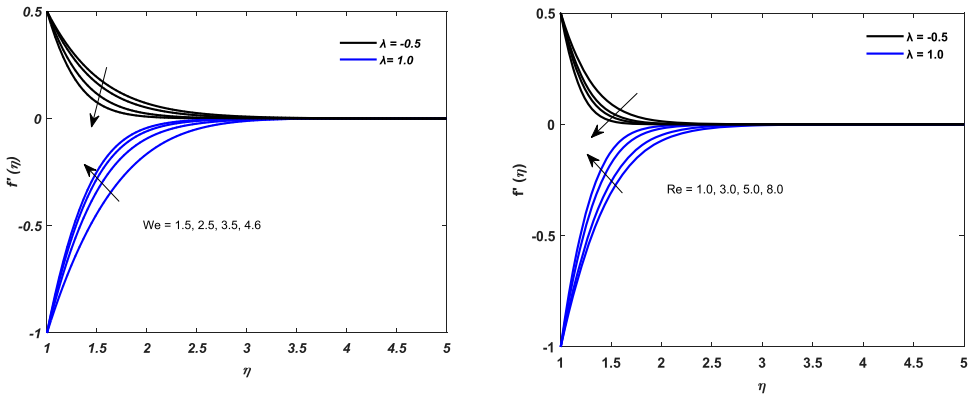


Figure 2. (a,b): Demonstration of  $We$  and  $Re$  of the velocity field for stretching and shrinking the cylinder.

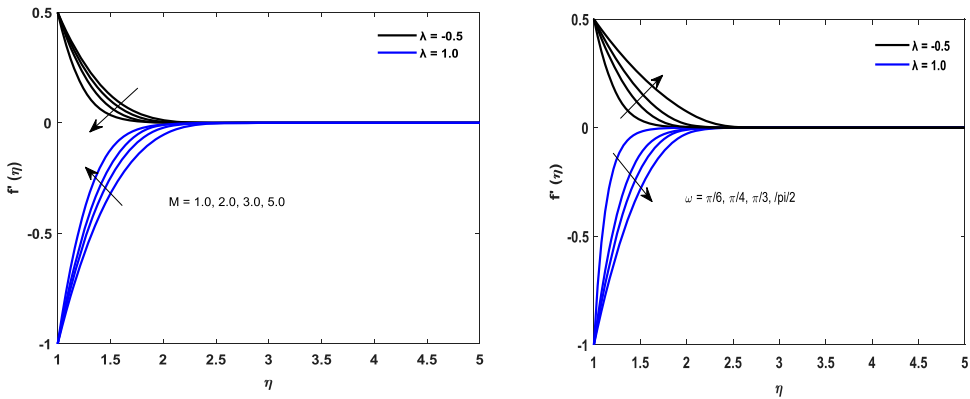


Figure 3. (a,b): Demonstration of  $M$  and  $\omega$  of the velocity field for stretching and shrinking the cylinder.

### 5. Debate on numerical outcomes

This section presents the numerical outcomes obtained during the execution of the numerical technique. In this study, the execution of the inclination of a magnetic dipole, nanoscale exchange of heat with cylinder geometry is made to analyze the Cross Nanofluid. In the deep eye, it is observed that there is established a scheme for the solution of nonlinear higher order ODEs presented in Equations (13)–(15). Hence to reduce the order of ODEs the shooting scheme is applied. Furthermore, Bvp4c is applied to get the numerical simulations of the model. Weissenberg number is symbolized as  $We$ ,  $Pr$  for Prandtl number, Schmidt ratio is described as  $Sc$ , local Reynold number is represented as  $Re$ , etc. Pictorial explanations for the numerical results are shown in Figures 2–8. Statistical data are collected to check the manner of all physical parameters and quantities from graphs (9–17). The parameter obtained from the ratio between initial velocity and free stream velocity is  $\lambda$ , if  $\lambda < 0$  it is called the shrinking case and  $\lambda > 0$  gives the stretching case.

Equation of momentum, which shows the velocity magnitude of Cross nanofluid, is attached with  $We$ ,  $n$ ,  $Re$ ,  $A$ ,  $M$ , and  $\omega$  parameters. All necessary graphs and statistical pictures show the effects of the velocity of the Cross nanofluid.

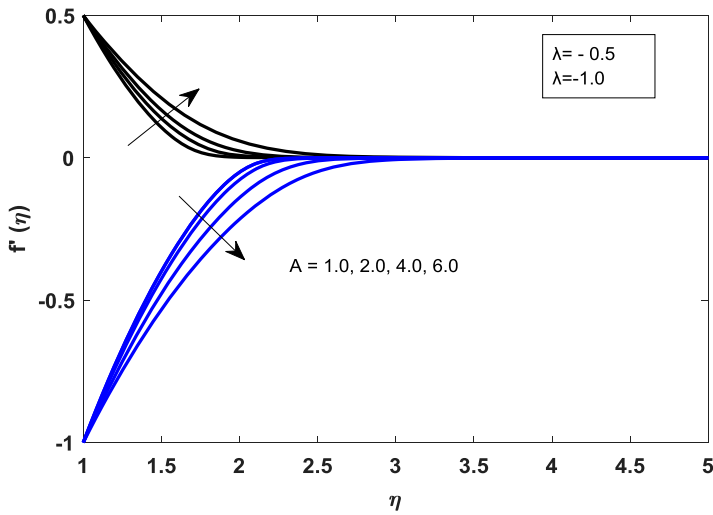


Figure 4. Demonstration of A of the velocity field for stretching and shrinking the cylinder.

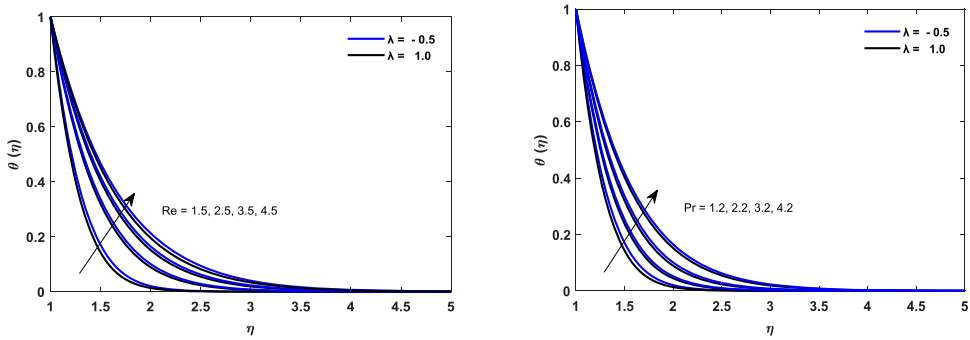


Figure 5. (a,b): Demonstration of Re and Pr of temperature field for stretching and shrinking the cylinder.

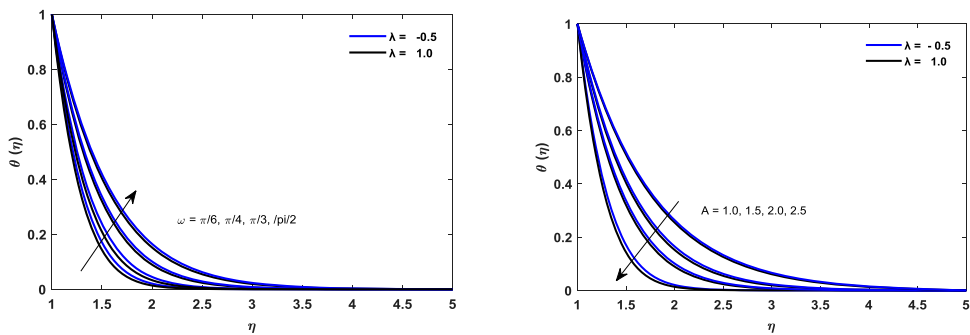
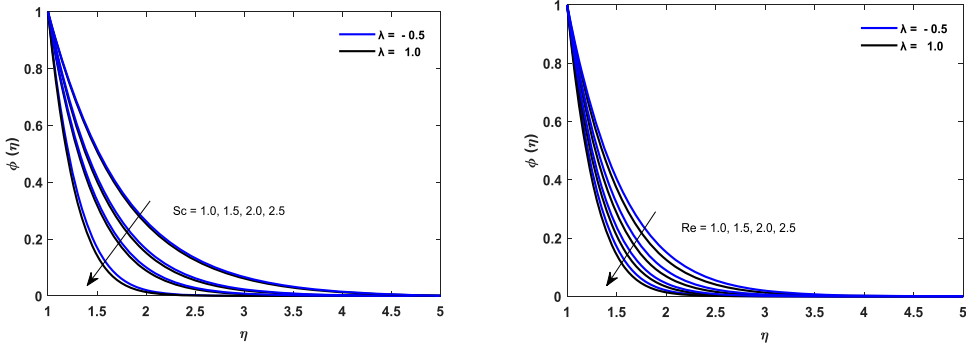
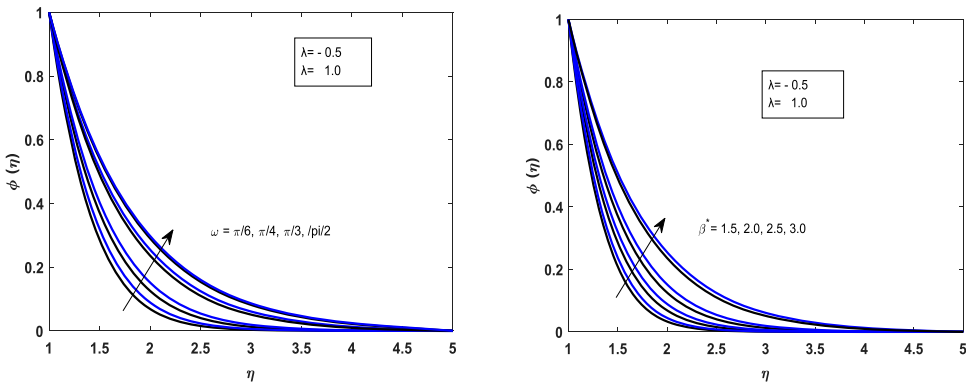


Figure 6. (a,b): Demonstration of  $\omega$  and A of temperature field for stretching and shrinking the cylinder.



**Figure 7.** (a,b): Demonstration of  $Sc$  and  $Re$  of mass transfer field for stretching and shrinking the cylinder.



**Figure 8.** (a–b): Demonstration of  $\omega$  and  $\beta^*$  of the velocity field for stretching/shrinking the cylinder.

When cylinder shrinks, then velocity becomes higher and due to relaxation of time factor, velocity field goes down for the shrinking case and gets higher for the stretching case. Velocity distribution gets fast for  $Re$  in the case of stretching and the opposite attitude is shown for the shrinking cylinder. Physically,  $Re$  is the ratio between viscous forces and inertial forces and greater  $Re$  results greater inertial forces. As in the case of stretching cylinder, inertial forces become lose and velocity gets fast speed while for the shrinking cylinder these forces become stronger and play an obstacle role in flow due to this flow, the velocity gets down. Demonstration of  $We$  and  $Re$  of velocity field for stretching and shrinking cylinder is shown in Figure 2(a,b). Figure 3(a,b) demonstrates the physical impact of  $M$  and  $\omega$  of velocity field for stretching and shrinking cylinder. Both parameters produce Lorentz force and due to this, the velocity gets down. As Lorentz force is the combination of electric and magnetic force and they both retard the flow speed, hence the velocity is decreased. Figure 4 shows the demonstration of  $A$  of the velocity field for stretching and shrinking the cylinder. Figure 5(a,b) demonstrates the physical impact of  $Re$  and  $Pr$  on the temperature field for stretching and shrinking the cylinder.  $Pr$  increases the thermal thickness because this factor temperature of the Cross fluid is goes up for both cases. Figure 6(a,b) demonstrates  $\omega$  and  $A$  of temperature field for stretching and shrinking the cylinder. The inclination angle reduces the velocity due to which the temperature of the Cross nanofluid increases rapidly.

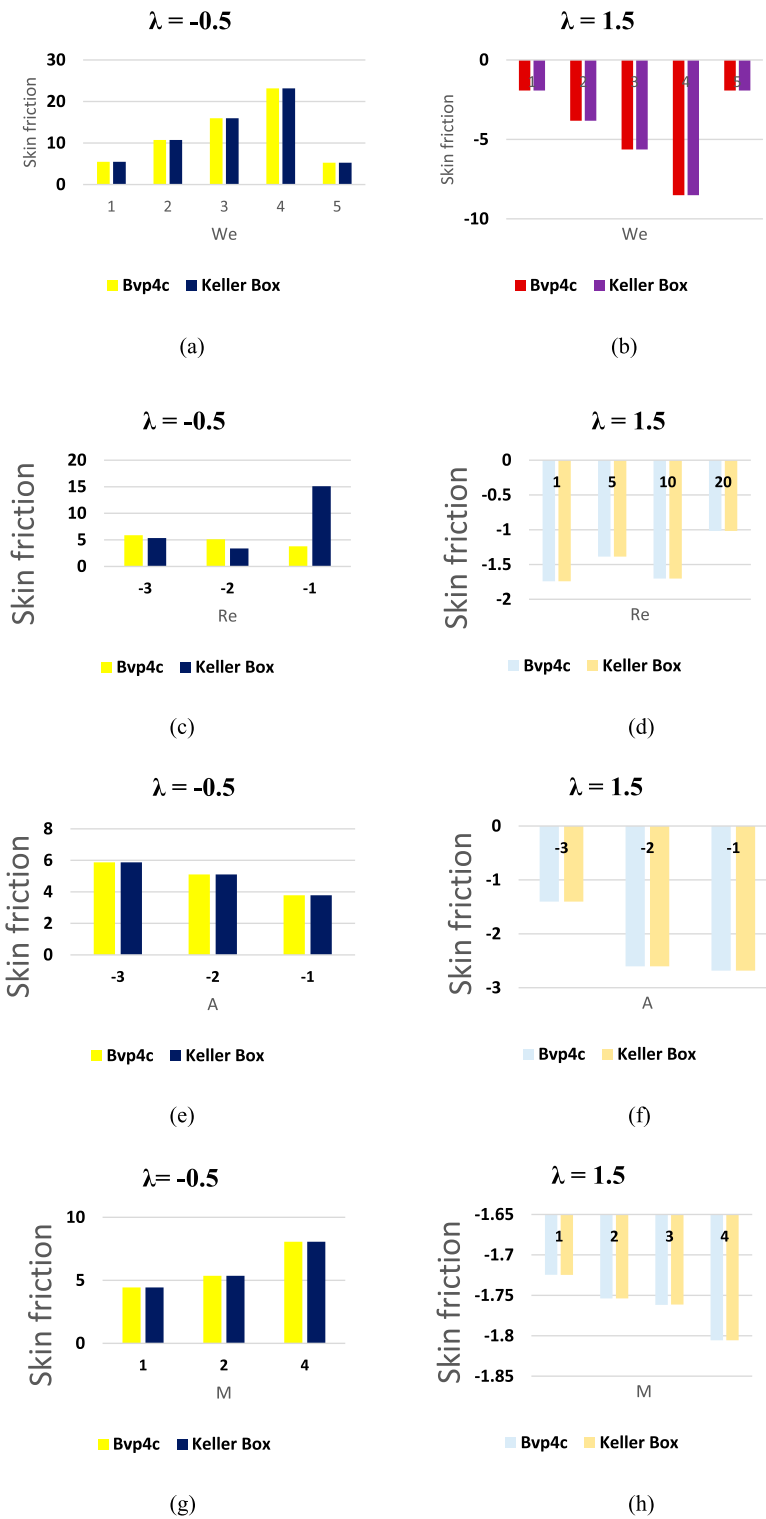
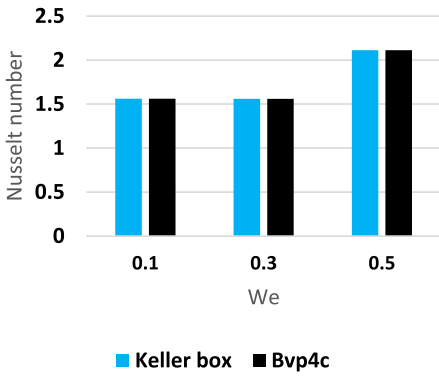
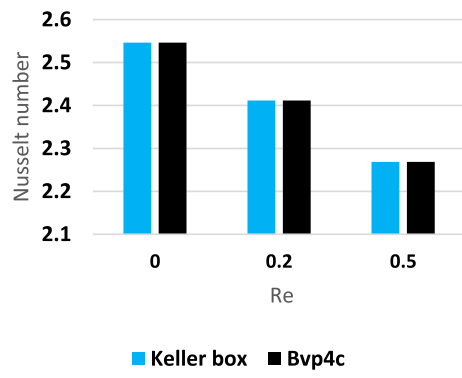


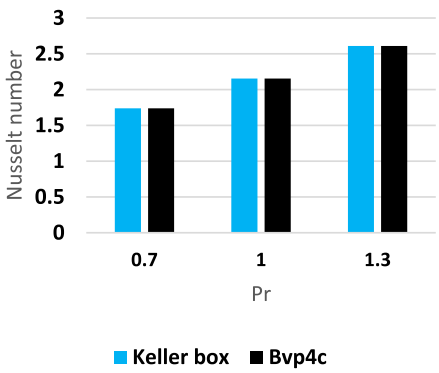
**Figure 9.** (a–h): Demonstration of skin friction for shrinking/stretching case for various physical parameters We, Re, A, and M.



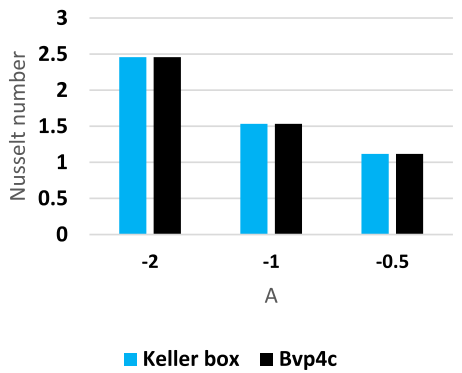
(a)



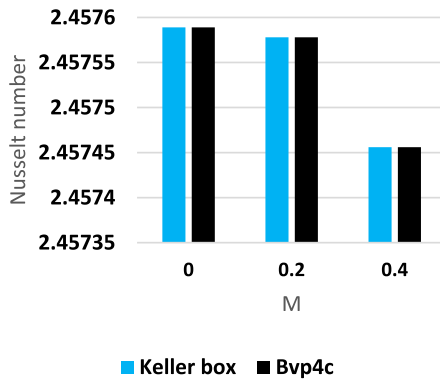
(b)



(c)



(d)



(e)

**Figure 10.** (a–e): Demonstration of We, Re, Pr, A, and M with the Nusselt number.

Figure 7(a,b) demonstrates the  $Sc$  and  $Re$  of the mass transfer field for stretching and shrinking the cylinder. In both cases, these physical parameters are responsible for lower transportation of mass, while Figure 8(a,b) shows the inclination angle and  $\beta^*$  cause growth in the mass transfer field for stretching and shrinking the cylinder. Graphs (9–17) show the physical parameters are linked with the physical quantities. Figures 9 and 10

## 6. Concluding remarks

The nanoscale heat transporting phenomenon of the fluid is explored by including the Lorentz force and variable thermal conductivity with the mathematical model of the cross model. The Cross fluid helps to investigate the problem in the shear thinning/thickening region. The numerical representations of the problem are provided via the BVP4C scheme.

The concluding remarks of this study are provided as follows:

1. Thermal conductivity enhances the nanoscale transport of energy.
2. Incline angle parameters produce the Lorentz force and due to which the velocity gets down.
3. Due to the relaxation of the time factor velocity field goes down for the shrinking case and higher for the stretching case for the 'We' physical parameter.
4. Velocity distribution gets rapid for  $Re$  in the case of stretching and the opposite attitude is shown for the shrinking cylinder.
5. The designed model is successfully solved using numerical procedures based on the BVP4C.
6.  $Pr$  increases thermal thickness due to which factor temperature of the Cross fluid goes up for both cases.
7. The inclination angle reduces the velocity due to which factor temperature of the Cross nanofluid increases rapidly.

## Disclosure statement

The authors declare that they have no known competing financial interests or personal relationships that could have appeared to influence the work reported in this paper.

## ORCID

Mohamed R. Ali  <http://orcid.org/0000-0002-0795-0709>

## References

- [1] Waqas M, Khan MI, Hayat T, et al. Transportation of radiative energy in viscoelastic nanofluid considering buoyancy forces and convective conditions. *Chaos, Solitons Fractals*. 2020;130:109415.
- [2] Yang L, Du K, Zhang Z. Heat transfer and flow optimization of a novel sinusoidal minitube filled with non-Newtonian SiC/EG-water nanofluids. *Int J Mech Sci*. 2020;168:105310.
- [3] Komeilibrjandi A, Raffiee AH, Maleki A, et al. Thermal conductivity prediction of nanofluids containing CuO nanoparticles by using correlation and artificial neural network. *J Therm Anal Calorim*. 2020;139(4):2679–2689.
- [4] Yang L, Huang JN, Ji W, et al. Investigations of a new combined application of nanofluids in heat recovery and air purification. *Powder Technol*. 2020;360:956–966.

- [5] Puneeth V, Manjunatha S, Makinde OD, et al. Bioconvection of a radiating hybrid nanofluid past a thin needle in the presence of heterogeneous–homogeneous chemical reaction. *J Heat Transfer*. 2021;143(4):042502.
- [6] Sabir Z, Ayub A, Guirao JL, et al. The effects of activation energy and thermophoretic diffusion of nanoparticles on steady micropolar fluid along with Brownian motion. *Adv Mater Sci Eng*. 2020;2020.
- [7] Ayub A, Wahab HA, Sabir Z, et al. A note on heat transport with aspect of magnetic dipole and higher order chemical process for steady micropolar fluid. In *Fluid-structure interaction*. IntechOpen (2020).
- [8] Shah SZH, Ayub A, Sabir Z, et al. Insight into the dynamics of time-dependent cross nanofluid on a melting surface subject to cubic autocatalysis. *Case Stud Therm Eng*. 2021;27:101227.
- [9] Wahab HA, Hussain Shah SZ, Ayub A, et al. Multiple characteristics of three-dimensional radiative Cross fluid with velocity slip and inclined magnetic field over a stretching sheet. *Heat Transfer*. 2021;50(4):3325–3341.
- [10] Ayub A, Wahab HA, Shah SZ, et al. Interpretation of infinite shear rate viscosity and a nonuniform heat sink/source on a 3D radiative cross nanofluid with buoyancy assisting/opposing flow. *Heat Transfer*. 2021;50(5):4192–4232.
- [11] Ayub A, Sabir Z, Le DN, et al. Nanoscale heat and mass transport of magnetized 3-D chemically radiative hybrid nanofluid with orthogonal/inclined magnetic field along rotating sheet. *Case Stud Therm Eng*. 2021;26:101193.
- [12] Ayub A, Darvesh A, Altamirano GC, et al. Nanoscale energy transport of inclined magnetized 3D hybrid nanofluid with Lobatto IIIA scheme. *Heat Transfer*. 2021;50(7):6465–6490.
- [13] Shah SZ, Wahab HA, Ayub A, et al. Higher order chemical process with heat transport of magnetized cross nanofluid over wedge geometry. *Heat Transfer*. 2021;50(4):3196–3219.
- [14] Ayub A, Wahab HA, Hussain Shah SZ, et al. On heated surface transport of heat bearing thermal radiation and MHD Cross flow with effects of nonuniform heat sink/source and buoyancy opposing/assisting flow. *Heat Transfer*. 2021;50(6):6110–6128.
- [15] Ayub A, Sabir Z, Altamirano GC, et al. Characteristics of melting heat transport of blood with time-dependent cross-nanofluid model using Keller–Box and BVP4C method. *Eng Comput*. 2022;38(4):3705–3719.
- [16] Shah SZH, Fathurrochman I, Ayub A, et al. Inclined magnetized and energy transportation aspect of infinite shear rate viscosity model of Carreau nanofluid with multiple features over wedge geometry. *Heat Transfer*. 2022;51(2):1622–1648.
- [17] Haider A, Ayub A, Madassar N, et al. Energy transference in time-dependent Cattaneo–Christov double diffusion of second-grade fluid with variable thermal conductivity. *Heat Transfer*. 2021;50(8):8224–8242.
- [18] Reddy CS, Ali F, Ahmed MFAF. Aspects on unsteady for MHD flow of Cross nanofluid having gyrotactic motile microorganism due to convectively heated sheet. *Int J Ambient Energy*. 2021:1–33. (just-accepted).
- [19] Waqas H, Khan SA, Khan SU, et al. Falkner–Skan time-dependent bioconvection flow of cross nanofluid with nonlinear thermal radiation, activation energy and melting process. *Int Commun Heat Mass Transfer*. 2021;120:105028.
- [20] Imran M, Farooq U, Waqas H, et al. Numerical performance of thermal conductivity in bioconvection flow of cross nanofluid containing swimming microorganisms over a cylinder with melting phenomenon. *Case Stud Therm Eng*. 2021;26:101181.
- [21] Noor NFM, Hashim I. MHD viscous flow over a linearly stretching sheet embedded in a non-Darcian porous medium. *J Porous Media*. 2010;13(4):349–355.
- [22] Noor NFM. Faculty of applied science and mathematics Universiti Industri Selangor, 45600 Bestari Jaya, Selangor, Malaysia Ishak Hashim\* centre for modeling & data analysis. *Sains Malaysiana*. 2009;38(4):559–565.
- [23] Xiong PY, Hamid A, Chu YM, et al. Dynamics of multiple solutions of Darcy–Forchheimer saturated flow of Cross nanofluid by a vertical thin needle point. *Euro Phys J Plus*. 2021;136(3):1–22.



- [24] Hafeez A, Yasir M, Khan M, et al. Buoyancy effect on the chemically reactive flow of Cross nanofluid over a shrinking surface: dual solution. *Int Commun Heat Mass Transfer*. 2021;126:105438.
- [25] Li YX, Mishra SR, Pattnaik PK, et al. Numerical treatment of time dependent magnetohydrodynamic nanofluid flow of mass and heat transport subject to chemical reaction and heat source. *Alexandria Eng J*. 2022;61(3):2484–2491.
- [26] Yu B, Ramzan M, Riasat S, et al. Impact of autocatalytic chemical reaction in an Ostwald-de-Waele nanofluid flow past a rotating disk with heterogeneous catalysis. *Sci Rep*. 2021;11(1):1–17.
- [27] Gul H, Ramzan M, Chung JD, et al. Multiple slips impact in the MHD hybrid nanofluid flow with Cattaneo–Christov heat flux and autocatalytic chemical reaction. *Sci Rep*. 2021;11(1):1–14.
- [28] Wang F, Sajid T, Ayub A, et al. Melting and entropy generation of infinite shear rate viscosity Carreau model over Riga plate with erratic thickness: a numerical Keller Box approach. *Waves Random Complex Media*. 2022:1–25.
- [29] Shah SL, Ayub A, Dehraj S, et al. Magnetic dipole aspect of binary chemical reactive Cross nanofluid and heat transport over composite cylindrical panels. *Waves Random Complex Media*. 2022:1–24.
- [30] Ayub A, Sabir Z, Shah SZH, et al. Aspects of infinite shear rate viscosity and heat transport of magnetized Carreau nanofluid. *Euro Phys J Plus*. 2022;137(2):1–17.
- [31] Ayub A, Shah SZH, Sabir Z, et al. Spectral relaxation approach and velocity slip stagnation point flow of inclined magnetized cross-nanofluid with a quadratic multiple regression model. *Waves in Random and Complex Media*. 2022:1–25.
- [32] Ayub A, Wahab HA, Balubaid M, et al. Analysis of the nanoscale heat transport and Lorentz force based on the time-dependent Cross nanofluid. *Eng Comput*. 2022:1–20.
- [33] Ayub A, Sabir Z, Shah SZH, et al. Effects of homogeneous-heterogeneous and Lorentz forces on 3-D radiative magnetized cross nanofluid using two rotating disks. *Int Commun Heat Mass Transfer*. 2022;130:105778.